



ISSN: 0067-2904

Green Synthesis of Iron Oxide Nanoparticles and Their Modification with CTAB for the Decolorization of Dye Reactive Blue 238

Hasan Fadhil Al- Rubai*, Atyaf Khalid Hameed Al-dahan, Ban A.Jasim
Ministry of Science and Technology, Environment and Water Directorate, Baghdad, Iraq

Received: 5/12/2021

Accepted: 30/8/2022

Published: 30/4/2023

Abstract

Magnetized iron oxide nanoparticles (NPs) were prepared using Eucalyptus leaf extract and then coated with CTAB (Cetrimonium bromide) to increase efficiency. The prepared and modified (NPs) were characterized using AFM, FTIR, and X-ray techniques. The adsorption of the dye reactive blue RB 238 on coated (NPs) was investigated. The effect of various experimental factors, such as the initial concentration of the dye, the amount of adsorbent, pH and temperature on the removal of RB238 was studied. The best conditions for dye removal were found to be 298 K in an acidic medium of pH = 3 and an appropriate dose of the adsorbent of 0.15 g per 25 mg/L to achieve the best color removal of 90% within 60 minutes. The pseudo-second-order reaction model gave results more suitable for experimental facts than the pseudo-first-order reaction model.

Keywords: Adsorption, Decolorization, Modified nanoparticles, Treatment.

التوليف الاخضر لأكسيد الحديد النانوي وتعديله باستخدام الستريمونيوم برومايد لازالة لون الصبغة الزرقاء الفعالة

حسن فاضل الربيعي*، أطياف خالد الدهان، بان عبد الوهاب جاسم

دائرة البيئة والمياه، وزارة العلوم والتكنولوجيا، بغداد، العراق

الخلاصة

تم تحضير الجسيمات النانوية لأكسيد الحديد الممغنط باستخدام مستخلص ورق الكالبتوز ثم تم تدعيمها بواسطة الستريمونيوم برومايد لزيادة الكفاءة. تم توصيف الدقائق النانوية باستخدام تقنيات مثل مجهر القوة الذرية، مطيافية الأشعة تحت الحمراء وحيود الأشعة السينية. تم التحقيق في امتزاز الصبغة الزرقاء الفعالة 238 على الدقائق النانوية. تمت دراسة تأثير العوامل التجريبية المختلفة مثل التركيز الأولي للصبغة وكمية الممتزات ودرجة الحموضة ودرجة الحرارة. أن أفضل الظروف لازالة الصبغة هي 298 K ووسط حامضي باس هيدروجيني يساوي 3، اما الجرعة المناسبة من المادة الممتزة هي 0.15 غم لكل 25 ملغم / لتر لتحقيق افضل ازالة بنسبة 90% خلال 60 دقيقة. أعطى نموذج تفاعل من الدرجة الثانية الكاذب نتائج اكثر ملائمة للحقائق التجريبية من نموذج تفاعل الكاذب من الدرجة الأولى.

*Email: hasanfalrubai66@gmail.com

1. Introduction

Wastewater treatment has always been a major concern of environmental advocates. [1]. Dye pollutants are the main cause of pollution. Reactive dyes are widely used in the textile industry as basic materials due to the ability of the active groups in their composition to bind to textile fibers using covalent bonds [2]. There is a large loss of non-fixable dyes in the wastewater because the stabilization efficiency of reactive dyes ranges between 60 and 90% in the dyeing process, and it's believed there will be high loads of organic pollutants. This will obviously increase the value of the chemical demand for oxygen, the decrease in the biological decomposition, and the high salt level [3]. The dye reactive blue 238 (RB238) is used as a coloring agent for textiles and leather. The presence of residues of this dye in wastewater causes cancerous tumors, respiratory problems, and allergies. This dye is highly soluble in water, so it can be difficult to remove with common chemicals [4]. Recently, nanomaterials have attracted the great interest of researchers because of their distinctive properties. They have been used in various scientific fields, including biomedical, environmental sciences, and engineering [5]. One of the effective nanomaterials is the porous metal oxides that are used for wastewater treatment. This is due to the advantage of these solids in the presence of sufficient active surface sites in addition to their high surface area [6]. Cementing magnetic nanoparticles is a major challenge and a key to various applications that can be accomplished through the physical or chemical adsorption of organic compounds [7]. Numerous reports and research have been published on the use of buffer nanoparticles and dye separation. This includes the decomposition of RR15 dye by kaolinite supported zero valent iron [8], the removal of orange II by the carbon-modified TiO_2 [9], and the use of magnetic ZnFe_2O_4 spinel ferrite nanoparticles in the decomposition of dye solutions acid red 88 [10]. Also, the adsorption of azo dye acid orange 7 in zero valent iron activated with potassium persulphate, acid dye adsorption on bentonite modified by acetyl trimethyl ammonium bromide [11], and the development of (NPs) activated carbon for the removal of (Cr, Cu, and Cd) from aqueous solutions [12]. The following investigation presents a simple, fast, more economical and efficient method for removing RB238 using magnetized iron oxide coated with CTAB. It is an environmentally friendly method as it does not leave residues that are difficult to dispose of.

2. Materials and methods

Materials

Reactive blue (RB238) was obtained from [Ciba unique chemical compounds] and has been used without additional purification. Cetrimonium bromide ($\text{C}_{19}\text{H}_{42}\text{BrN}$, CTAB) was obtained from Chuchardt (Germany). NaOH and H_2SO_4 have been used to modify the pH, which was purchased from Appli Chem (GmbH). FeCl_3 was obtained from Fluka. Eucalyptus leaves from the gardens of the Ministry of Science and Technology. All solutions were prepared using distilled water.

Preparation of NPs using Eucalyptus leaf extracts and supported by CTAB

Iron oxide nanoparticles (Fe_3O_4 -NPs) were prepared *via* the chemical precipitation method [13]. First, eucalyptus leaves are collected and washed well before being heated at 80 °C for 30 minutes. The ratio of the leaf weight to the distilled water volume was 100 gm/L. The extract was then separated by filtration and left in a cool place (the pH of the extract was 4). Second, to prepare NPs (20 mL) of the extract, they were slowly added to an aqueous solution of FeCl_3 (0.01 M) at a ratio of 1:2, with stirring at room temperature for 3 minutes. The color of the yellow aqueous solution changed to greenish-black, which indicates the deposition of NPs. The nanoparticles were filtrated and washed several times with distilled water. The pH of the resulting solution after washing was changed to 11, where 500 mL was

prepared in a suspension with a concentration of 10 mg/L and saved for use in the next step. Third, CTAB solution (50 mL, 0.1 gm/10 mL) was added to the solution in step 2, with continuous stirring for 30 minutes. Finally, the desired nanoparticles were filtrated and dried at 50 °C for one hour.

Batch experiments

Adsorption of RB238 on a modified CTAB is turned into a batch gadget. RB238 solution (100 mL, 25-75 mg/L) in a conical flask. The aggregate was shaken using a thermostatically controlled shaker right away. The shaker velocity was fixed at one hundred fifty rpm. The samples were taken (10 mL) at precise time periods (5, 10, 15, 20, 30, 45 and 60 minutes). The dye solution was removed by the adsorbent, and evaluated for the coloration elimination efficiencies at $\lambda_{\max} = 610$ nm using ultraviolet and visible spectroscopy (Japan; Optima Model SP-3000; UV/VIS) geared with a quartz cell of 1.0 cm path duration.

Techniques used to determine the properties of adsorbents

Atomic Force Microscopy (AFM) measures the contact force between the tip and surface by the method of detection using a laser and position-sensitive photodiode detector (NT-MDT-Ntegra-Russian Federation). A Fourier transformed infrared spectrophotometer (FT-IR Prestige-21 Shimadzu) was used in the range of 4000-500 cm^{-1} with KBr pellets. The X-ray diffraction (XRD) patterns of the sample were measured by Shimadzu Corporation Lab-X (XRD-6000) and recorded in the range of 3-80 degrees with a speed of 5.0 deg min^{-1} and a preset time of 0.6 second.

3. Results and discussion

Analysis and calculation

The degradation efficiency of RB238 was studied using the following relationship: Decolorization efficiency

$$\% = [(C_0 - C_t) / C_0] \times 100 \% \quad (1)$$

Where C_0 (mg.L^{-1}) is the initial dye concentration, and C_t (mg.L^{-1}) is the concentration of dye at the reaction time t (min.). The amount of dye (RB238) adsorbed per unit mass of adsorbent q_t (mg.g^{-1}) can be expressed as follows:

$$q_t = (C_0 - C_t) V / W \quad (2)$$

Where W (g) is the mass of the adsorbent and V (L) is the volume of the solution under investigation. To match the experimental data gathered during the dye breakdown, two types of reaction kinetics, the first and the second pseudo have been used to study the kinetics of the RB238 dye decolorization reaction. The pseudo-first-order model is given by equation 3 [14].

$$\log (q_e - q_t) = \log q_e - k_1 * t / 2.303 \quad (3)$$

Where q_t (mg.g^{-1}) is the adsorption ability at time t , q_e (mg.g^{-1}) is the potential at equilibrium, and k_1 (min^{-1}) represents the rate constant of the pseudo-first order version. The pseudo-second order reaction is given by equation 4 as follows [15].

$$t / q_t = 1 / k_2 q_e^2 + t / q_e \quad (4)$$

Where k_2 ($\text{Lmg}^{-1} \cdot \text{min}^{-1}$) is the rate constant of the pseudo-second order model.

Adsorbent characterize

FT-IR spectroscopy was used to collect accurate spectroscopic data about the general composition of the NPs (Figure 1) after CTAB coating. The peak at 571 cm^{-1} belongs to the Fe-O vibration of the NPs. The two peaks at 2924 and 2859 cm^{-1} are attributed to the

vibrations of the C-H bond of CTAB [12]. The absorption at 2376 cm^{-1} , may be due to the unsaturated group C=N of the plant leaf extract. The absorptions of 3433 cm^{-1} and 1634 cm^{-1} for O-H stretching and bending vibrations, respectively, were due to the surface of the OH group of the CTAB loaded nanoparticles [16].

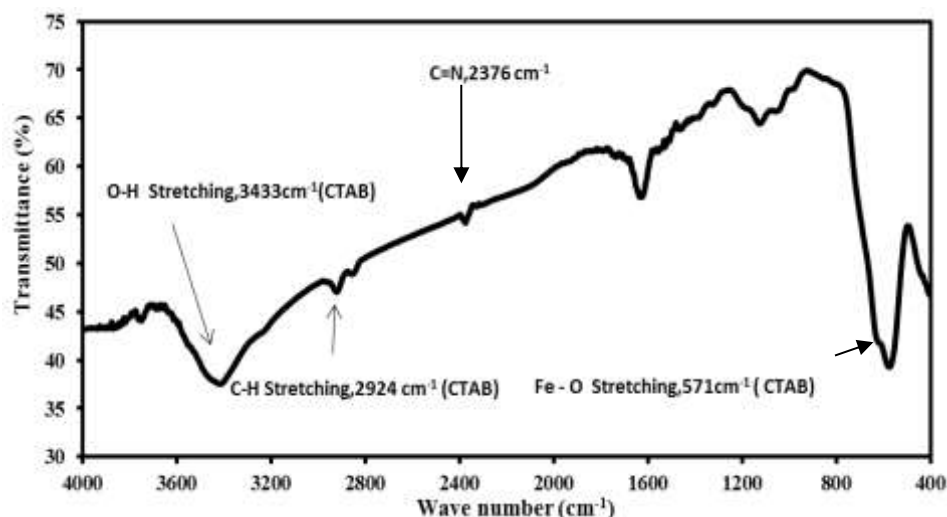


Figure 1: FT-IR spectrum of Fe_3O_4 coating CTAB

AFM images 2a, 2b and 2c showed a change in the size of nanoparticles after being coated with CTAB. In Figure 2a, the pure NPs have a size of about 55 nm, while in Figure 2b, the size is about 40 nm after being coated with CTAB. Additionally, there is a significant improvement in the number of nanoparticles that have a size smaller than 40 nm. There is a good impression from FT-IR spectra that the surface of the nanoparticles is well coated.

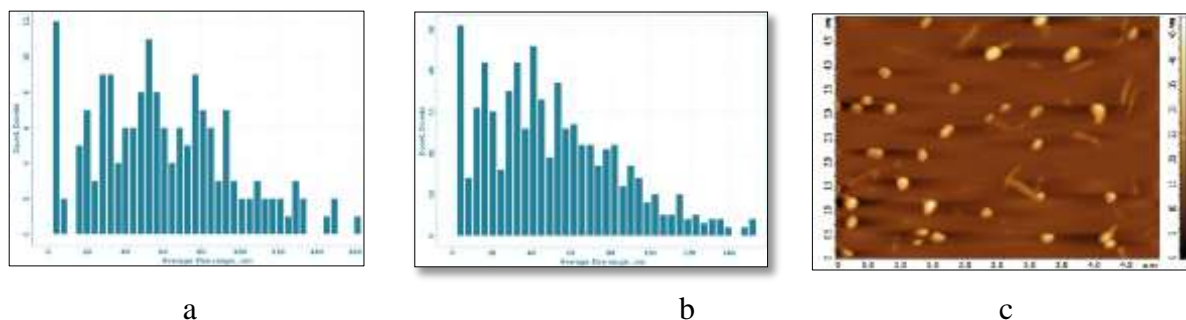


Figure 2: AFM photomicrograph of Fe_3O_4 NPs: (a) Line graph of pure NPs (b) Line graph of NPs coating by CTAB (c) 3D topography of NPs coating by CTAB

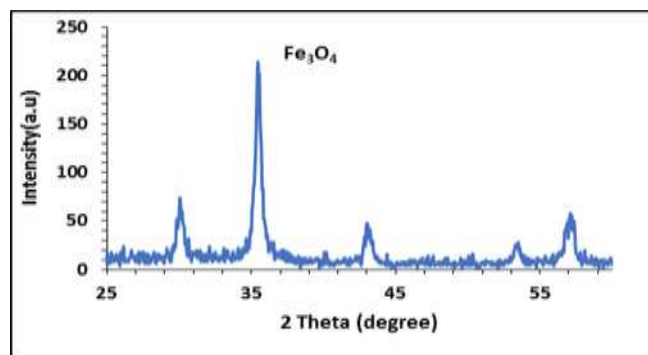


Figure 3: XRD of Fe_3O_4 (NPs)

Figure 2c is a three-dimensional image of the nanoparticles after being coated. As shown in Figure 3, X-ray diffraction was used to examine the crystal phase of Fe_3O_4 nanoparticles.

Effect of different factors on the decolorization efficiency of RB238

Effluence of adsorbent dosage

Figure 4 shows the effect of changing the NPs modified dose on the decolorization efficiency of the dye solution. It was found that the efficiency of removal of the color increases with the increase of the nanoparticles coated dose, but it is not necessary to use a dose greater than 150 mg because the decolorization efficiency was not greatly affected. When the dose of NPs-coated is 150 mg, the efficiency of color removal reaches 90%. Thus, this amount of modified NPs has been used for the next experiments.

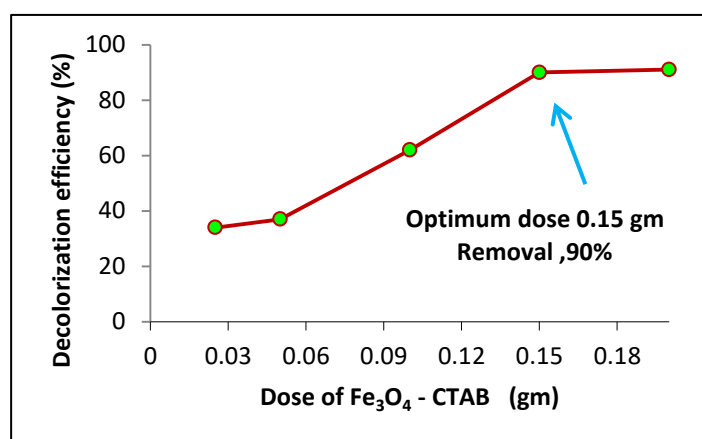


Figure 4: Effect of the adsorbent dosage on decolorization efficiency (temperature = 298 K, pH = 3, rpm = 150, contact time = 60 min, and RB238 concentration = 25 mg.L^{-1}).

Effluence of pH

The pH values of 3, 6 and 9 were chosen to investigate the effect of pH on the adsorption capacity of CTAB coated nanoparticles. Figure 5 shows the decomposition efficiencies of 82, 53 and 51% at pH values of 3, 6, and 9, respectively, at a contact time of 45 minutes. It is likely that the lower removal efficiency with increasing pH is due to the effect of pH on the surface charge of the adsorbent and the degree of ionization of the adsorbents [17].

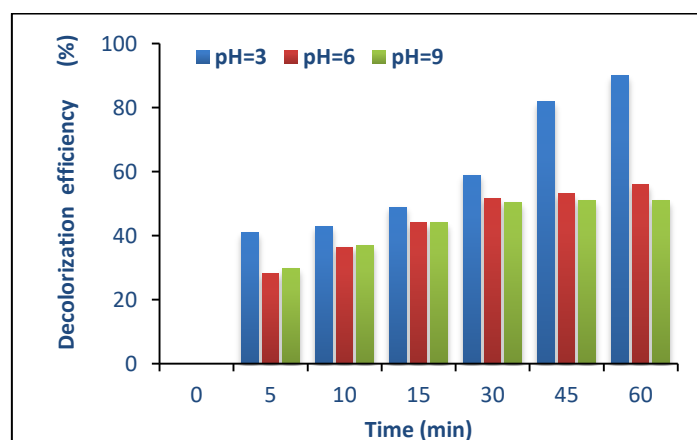


Figure 5: Effect of initial pH on decolorization efficiency (temperature = 298 K, adsorbent dosage = 0.15 g rpm = 150, and RB238 concentration = 25 mg.L^{-1}).

As long as there is a change in the efficiency of decolorization in the acid and base media, this means there are two different mechanisms in the adsorption process, because both the adsorbent and the adsorbed substances have an ionic structure. On the other hand, the decrease in the removal percentage in the alkaline medium is due to the similarity of the negative surface of the coated nanoparticles with the negative charge of the dye, which caused the repulsion of the two surfaces, decreased adsorption, and decreased decomposition efficiency.

Effect of primary dye concentration

The preliminary concentration of dyes is a good parameter for sensitive inspiration. Therefore, it is vital to have a look at the effect of primary dye concentration, and the effects are shown in Figure 6. This figure indicates elevated color elimination performance with a decreased concentration of dye RB238. As the concentration of dye lowered from 75 to 25 mg.L⁻¹, the decolorization performance of the dye grew from 6 to 43% within 10 minutes of the adsorption process. The degradation performance of the dye was reduced as the preliminary concentration was increased. This brings about a settlement with a proposed positioned range of susceptible sites. Competitive adsorption might interact with the adsorption and degradation of contaminants on the surface of particles and further reduce the reaction velocity [18].

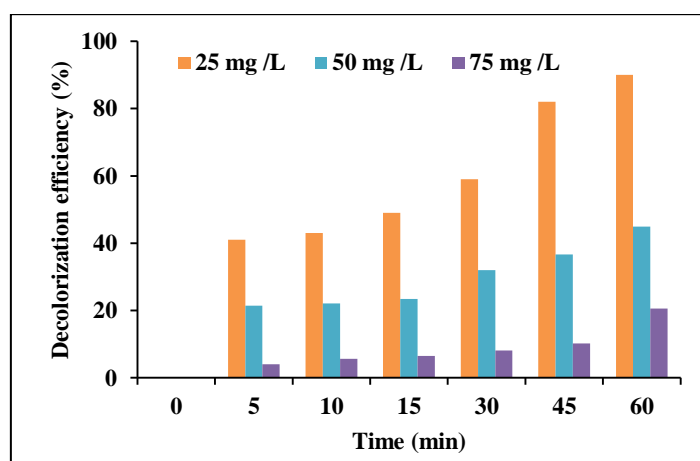


Figure 6: Effect of the variations of initial dye concentration on the decolorization efficiency (pH = 3.0, temperature = 298 K, adsorbent dosage = 0.15 g and rpm =150)

Effect of temperature

The effect of temperature on the adsorption process is an important parameter that should be studied. Figure 7 shows that 298 K is the best temperature to perform adsorption experiments for RB238 because it has got the highest percentage of color removal (90% in 60 minutes). There is no change in the efficiency of the degradation of the dye despite the increase in temperature to 308 K and 60 minutes of contact with the adsorbent. This type of adsorption could be exothermic [19,20].

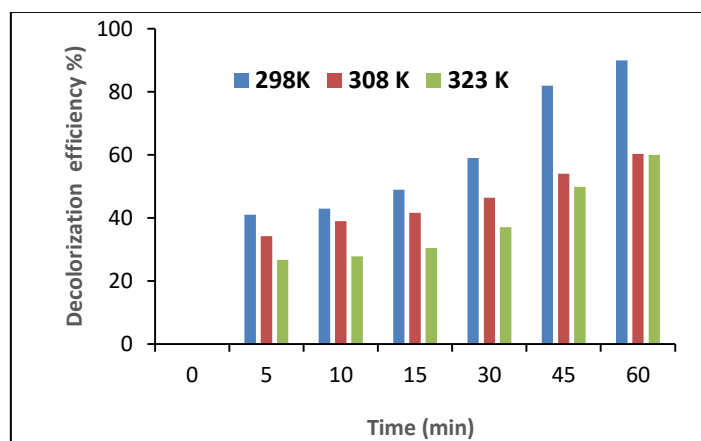


Figure 7: Influence of variations temperature on the decolorization efficiency (pH = 3.0, adsorbent dosage = 0.15 g, rpm = 150 and Rb238 concentration= 25 mg.L⁻¹)

Study of adsorption kinetics

Two kinetic models, pseudo-first and pseudo-second orders, have been used to fit the experimental data points obtained from the decolorization processes. An assessment of the consequences with a precise line is plotted in Figures 8 and 9, and the kinetic parameters are summarized in Table 1. The R^2 correlation coefficients of the pseudo-first order version are lower than the ones of the pseudo-second order model. The calculated (q_e) (the adsorption potential at equilibrium) appeared to be near the empirical values. This indicates that the pseudo-second order model version yields a higher match to the empirical data than the pseudo-first order model. Comparable outcomes were pronounced for the adsorption fees of AGYG, AB93, ATBA, and AB25 on B-A-CTAB [21].

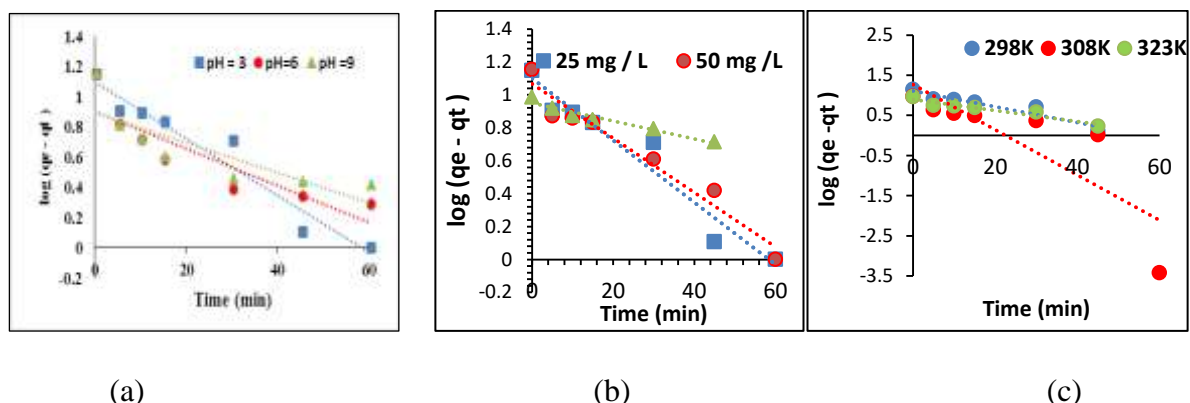


Figure 8 : Pseudo-first order kinetics plots of the adsorption of RB238 on Fe₃O₄ - CTAB at:
 (a) different pH values (b) diverse RB238 preliminary concentrations (c) various temperatures.

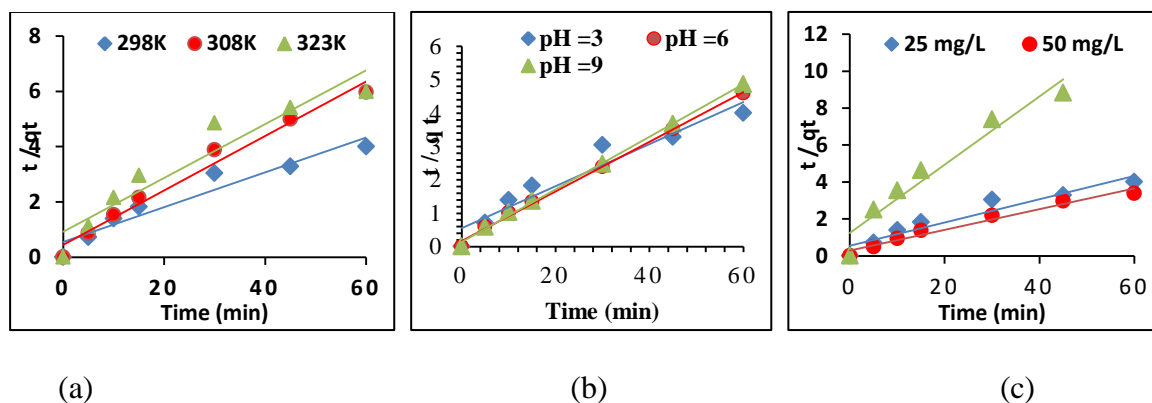


Figure 9 - Pseudo-second order kinetics plots of the adsorption of RB238 on Fe₃O₄ - CTAB at: (a) different pH values (b) diverse RB238 preliminary concentrations (c) various temperatures.

Table 1: The kinetic parameters of the reactive blue 238 on Fe₃O₄ (NPs)

T (k)	C ₀ (mg.L ⁻¹)	q _{e exp} (mg.g ⁻¹)	Pseudo-first order model			Pseudo-second order model		
			q _{1e} (mg.g ⁻¹)	k ₁ min ⁻¹	R ²	q _{2e} (mg.g ⁻¹)	k ₂ (g.mg ⁻¹ .min ⁻¹)	R ²
298	25	14.989	12.876	0.0454	0.8977	15.898	0.007	0.9252
308	-	10.048	16.872	0.1296	0.6922	10.163	0.021	0.9776
323	-	10.006	7.893	0.0315	0.9175	10.288	0.01	0.9351
298	50	17.762	11.65	0.0379	0.9550	17.857	0.01	0.9684
-	75	10.275	5.417	0.0126	0.9463	8.932	0.027	0.9522

4. Acknowledgment

The authors would like to thank and appreciate the Directorate of Materials Research, particularly the Center for Advanced Materials, for their research collaboration

References

- [1] M. A. Atiya, A. K. Hassan, and F. Q. Kadhim, "Green synthesis copper nanoparticles using tea leaves extract to removal ciprofloxacin (CIP) from aqueous media." *Iraqi J. Sci.*, vol. 62, no. 9, pp. 2833-2854, 2021.
- [2] I. Bibi, N. Nazar, S. Ata, M. Sultan, A. Ali, A. Abbas, K. Jilani, S. Kamal, F. M. Sarim, M. I. Khan, F. Jalal and M. Iqbal, "Green synthesis of iron oxides nanoparticles using pomegranate seeds extract and photo catalytic activity evolution for the degradation of textile dye." *J. Mater. Res. Technol.* vol. 8, no. 6, pp. 6115-6124, 2019.
- [3] B. Zargar, H. Parham and A. Hatamie, "Fast removal and recovery of amaranth by modified iron oxide magnetic nanoparticles." *Chemosphere.* vol. 76, no. 4 pp. 554-557, 2009.
- [4] A. Khudhair, H. Fadhil and H. Hassan, "The kinetic model for decolorization of commercial reactive red azo dye aqueous solution by the Fenton process and study the effect of inorganic salts." *Al-Nahrain Uni. J. Sci.*, vol. 21, no. 3, pp. 82-93, 2018.
- [5] N. N. Nassar, "Iron oxide nan adsorbents for removal of various pollutants from wastewater," An overview. *Application of adsorbents for water pollution control*, pp. 81-118, 2012.
- [6] M. K. Nodeh, G. N. Bidhendi, M. A. Gabris and S. Shahabddin, "Strontium oxide decorated iron oxide activated carbon nanocomposite a new adsorbent for removal of nitrate from well water." *J. Braz. Chem. Soc.*, vol. 31, no. 1, pp. 116-125, 2020.

- [7] R. Sahraei, K. Hemati and M. Ghaemy, "Adsorptive removal of toxic metals and cationic dyes by magnetic adsorbent based on functionalized grapheme oxide from water." *RSC Adv.*, vol. 6, no. 76, pp. 72487-72499, 2016.
- [8] S. Fang, N. Yang, M. Qiu and C. Huang, "Degradation of dye C.I.reactive red 15 in aqueous solution by kaolinite supported zero valent iron." *Nat. Environ. Pollut. Technol.*, vol. 18, no. 3, pp. 963-968, 2019.
- [9] S. Jafari, B. Tryba, E. Kusiak-Nejman, J. Kapica, A. Kozar and M. Sillanpaa. "The role of adsorption in the photo catalytic decomposition of orange II on carbon-modified TiO₂." *J. Mol. Liq.*, vol. 220, pp. 504-512, 2016.
- [10] W. Konicki, D. Sibera, E. Mijowska, Z. Lendzion and U. Narkiewicz, "Equilibrium and kinetic studies on acid dye Acid Red 88 adsorption by magnetic ZnFe₂O₄ spinel ferrite nanoparticles." *J. Colloid Interface Sci.*, vol. 398, pp. 152-160, 2013.
- [11] M. Qiu. "Degradation of azo dye acid orange 7 by zero valent activated with potassium persulphate." *Nat. Environ. Pollut. Technol.*, vol. 18, no. 1, pp. 197-201, 2019.
- [12] M. Jain, M. Yadav, T. Kohout, M. Lahtine and M. Sillanapaa, "Development of iron oxide activated carbon nanoparticles composite for the removal of Cr(VI), Cu(II) and Cd(II) ions from aqueous solution." *Water resources and industry*, vol. 20, pp. 54-74, 2018.
- [13] M. Balamurugan, S. Saravanan and T. Soga, "Synthesis of iron oxide nanoparticles by using Eucalyptus plant extract." *J. Sur. Sci. Nano. Tech.*, vol. 12, pp. 363-367, 2014.
- [14] E. Orucoglu and S. K. Hacıyakupoglu, "Bentonite modification with hexadecyl pyridinium and aluminum polyoxy cations and its effectiveness in Se(IV) removal." *J. Environ. Manage.*, vol. 160, pp. 30-38, 2015.
- [15] S. B. Wang and H. W. Wu, "Environmental-benign utilization of fly ash as low-cost adsorbents." *J. Hazard. Mater.* vol. 136, no. 3, pp. 482-501, 2006.
- [16] X. D. Dan, L. W. Yun, W. K. Wang, B. Y. Shan, L. Q. Wen, G. M. Fan and M. H. Zhu, "Hydroxy-aluminium and cetyltrimethyl ammonium bromide modified bentonite as adsorbent and its adsorption for orange II." *Desalination and Water Treatment*, vol. 94, pp. 244-253, 2017.
- [17] H.H.Kadhim, and K.A.Saleh. "Removing of copper ions from industrial wastewater using grapheme oxide / chitosan nanocomposite." *Iraqi J.Sci*, vol.63, no.5, pp.1894-1908, 2022.
- [18] J. Zhang and M. Qiu. "Adsorption kinetics and isotherms of copper ion in aqueous solution by bentonite supported nano scale zero iron." *Nat. Environ. Pollut. Technol.*, vol. 18, no. 1, pp. 269-274, 2019.
- [19] B. H. Hameed, A. A. Ahmad and N. Aziz, "Isotherms, kinetics and thermodynamics of acid dye adsorption on activated palm ash." *Chem. Eng. J.*, vol. 133, no. 1-3, pp. 195-207, 2007.
- [20] Y. Y. Muhi-Alden and K. A. Salah, "Removing of methylene blue dye from its aqueous solution using polyacrylonitrile/iron oxide/grapheneoxide." *Iraqi J. Sci.*, vol. 63, no. 6, pp. 2320-2330, 2022.
- [21] L. G. Yan, L. I. Qin, H. Q. Yu, S. Li, R. Shan and B. Du. "Adsorption of acid dyes from aqueous solution by CTMAB modified bentonite: Kinetic and isotherm modeling." *J. Mol. Liq.*, vol. 211, pp. 1074-1081, 2015.